Published in final edited form as:
Biochemistry. 2012 April 3; 51(13): 2706–2716. doi:10.1021/bi3000929.

Kinetically competing huntingtin aggregation pathways control amyloid polymorphism and properties

Murali Jayaraman[†,‡,§], **Rakesh Mishra**[†,‡], **Ravindra Kodali**[†,‡], **Ashwani K. Thakur**[†,‡,¥], **Leonardus M. I. Koharudin**[†], **Angela M. Gronenborn**[†], and **Ronald Wetzel**[†,‡,*]

[†]Department of Structural Biology, University of Pittsburgh School of Medicine, Pittsburgh, PA 15260

[‡]Pittsburgh Institute for Neurodegenerative Diseases, University of Pittsburgh School of Medicine, Pittsburgh, PA 15260

Abstract

In polyglutamine (polyQ) containing fragments of the Huntington's disease protein huntingtin (htt), the N-terminal 17 amino acid htt^{NT} segment serves as the core of α-helical oligomers whose reversible assembly locally concentrates the polyQ segments, thereby facilitating polyQ amyloid nucleation. A variety of aggregation inhibitors have been described that achieve their effects by neutralizing this concentrating function of the htt^{NT} segment. In this paper we characterize the nature and limits of this inhibition for three means of suppressing htt^{NT}-mediated aggregation. We show that the previously described action of htt^{NT} peptide-based inhibitors is solely due to their ability to suppress the htt^{NT}-mediated aggregation pathway. That is, under htt^{NT} inhibition, nucleation of polyQ amyloid formation by a previously described alternative nucleation mechanism proceeds unabated and transiently dominates the aggregation process. Removal of the bulk of the htt^{NT} segment by proteolysis or mutagenesis also blocks the htt^{NT}-mediated pathway, allowing the alternative nucleation pathway to dominate. In contrast, the previously described immunoglobulin-based inhibitor, the anti-htt^{NT} V_L 12.3 protein, effectively blocks both amyloid pathways, leading to stable accumulation of non-amyloid oligomers. These data show that the htt^{NT}-dependent and independent pathways of amyloid nucleation in polyQ-containing htt fragments are in direct kinetic competition. The results illustrate how amyloid polymorphism depends on assembly mechanism and kinetics, and have implications for how the intracellular environment can influence aggregation pathways.

The expanded CAG repeat diseases are a series of familial neurodegenerative conditions resulting from the expansion of a polyglutamine (polyQ) tract in a disease protein (1). While disease mechanisms remain obscure, the early cellular events are presumably triggered by pathogenic interactions between one or more cellular targets and either monomers or aggregates of the expanded polyQ protein (2). The polyQ repeat length dependence of both disease risk and disease onset (1) correlates with the repeat length dependence of aggregation onset (3, 4), and polyQ-containing aggregates are found in victims of each of

[*]Corresponding author: Department of Structural Biology, University of Pittsburgh School of Medicine, Rm. 2046 Biomedical Sciences Tower 3, 3501 Fifth Avenue, Pittsburgh, PA 15260. rwetzel@pitt.edu. phone (412) 383-5271. fax (412) 648-9008.
[§]Pharmaceutical Research and Development, Pfizer, Inc., Chesterfield, MO, USA
[¥]Department of Biological Sciences and Bioengineering, Indian Institute of Technology, Kanpur, Uttar Pradesh, INDIA.

SUPPORTING INFORMATION AVAILABLE

A figure containing additional EM images of aggregates, as well as a brief discussion of the provenance and significance of these aggregates, is included in a single pdf file as supporting information. These data characterize in more detail the appearance of "simple polyQ-type" aggregates as intermediates in htt^{NT}-inhibited reactions of htt$^{NT}Q_{30}P_6K_2$ peptides. This material is available free of charge via the Internet at http://pubs.acs.org.

these diseases (1, 5). The detailed structures of the toxic species and the identities of their cellular targets are not known.

As with many other aggregation disease proteins (6–11), polyQ proteins are able to form a number of polymorphic aggregates both *in vitro* and *in vivo* (2, 12, 13). Simple polyQ peptides, flanked by a few charged residues, undergo classical nucleated growth polymerization into amyloid fibrils without the intervention of the kind of non-amyloid oligomeric species often observed in amyloid formation by disease proteins like Aβ (2, 14, 15). In contrast, polyQ fused to some flanking sequences, such as the 17 amino acid N-terminus (htt^{NT}) of the Huntington's disease (HD) protein huntingtin (htt), exhibit early formation of roughly spherical oligomers lacking β-structure, and these oligomers play critical roles in the formation of mature polyQ-core amyloid (2, 16–18). Aggregates of a wide range of morphologies have been isolated from a HD tg mouse model (13), and it is a reasonable possibility that only some of these aggregate polymorphs might be toxic. If so, it becomes particularly important to understand how the cellular environment interacts with the polyQ protein sequence to direct the formation of different aggregate morphologies.

Previous studies uncovered evidence that different growth conditions give rise to aggregates of polyQ-containing htt fragments that exhibit different morphologies and cytotoxicities (19). More recently, it was demonstrated that aggregates isolated from a number of HD tg mouse models are capable of seeding polyQ aggregation *in vitro* (20), suggesting an amyloid-like morphology and consistent with toxicity mechanisms postulating recruitment of normal polyQ proteins into aggregates (21, 22). Alternatively, non-amyloid oligomeric forms of htt fragments might be the toxic agents, consistent with the current view of aggregate toxicity in other disease states (8–10, 23). However, there is also some recent indirect evidence against a toxic role for such oligomers, in that analogs of polyQ-containing htt fragments that appear to be only capable of forming non-amyloid oligomers (18) are not toxic when expressed in mammalian cells (24, 25). The open question as to the nature of the toxic species in HD emphasizes the importance of better understanding the htt aggregation pathway and how it might be impacted by interactions with other molecules.

In this paper we describe how the aggregation reactions and products of polyQ-containing htt fragment model peptides are modified by certain effector molecules and protein modifications relevant to the cellular environment. We find that some events that target the key role of the htt^{NT} segment can delay htt^{NT}-mediated polyQ aggregation, providing a window for the operation of the normally underrepresented aggregation pathway analogous to that for simple polyQ peptides. Another htt^{NT} targeting inhibitor, in contrast, completely blocks nucleation of amyloid by any mechanism, leading to the stable accumulation of large non-amyloid oligomers. The results show that polyQ-containing htt fragments are capable of engaging at least three aggregation pathways leading to different aggregate products, and that the relative kinetics of these pathways can be influenced by other molecules and interactions. Since the different pathways generate aggregates of different structures and properties, the possibility exists for modulating toxicity not only by eliminating aggregation but also by its redirection towards more benign aggregated products.

MATERIALS AND METHODS

Materials

Synthetic peptides were obtained in unpurified form from the Keck Biotechnology Center at Yale (http://keck.med.yale.edu/ssps/), and were HPLC purified and disaggregated using a combination of aggregate dissociation and ultracentrifugation, as described (26). In some peptides an F17W mutation is present; previously we found that this mutation has a negligible effect on aggregation (16). Acetonitrile, hexafluoroisopropanol (99.5%,

spectrophotometric grade), and formic acid were from Acros Organics, and trifluoroacetic acid (99.5%, Sequanal Grade) from Pierce.

General methods

The sedimentation assay (26), the ThT and 90° light scattering assays (27), and the nucleation kinetics analysis (14, 26), have been described. The isolation of aggregates for seeding analysis was conducted by centrifuging a reaction aliquot at 14800 rpm in an Eppendorf centrifuge at 4 ° C for 30 mins, washing the pellet 2–3 times with PBS, resuspending in buffer, and determining the aggregate concentration by an HPLC analysis of a formic acid dissolved aliquot, as described (26, 28). SEC was on a Superdex 75 10/200 column (GE Health Sciences) equilibrated in PBS on an Agilent 1200 isocratic HPLC system with a flow rate of 0.4 ml/min and elution monitored at 214 nm. The column was calibrated with aprotinin, cytochrome C, ribonuclease, ovalbumin and bovine serum albumin. In complex formation experiments, new peaks were characterized by analysis of 500 μL portions of the peak fractions on a reverse phase HPLC column with detection on an Agilent 1100 LC-MS system.

Electron microscopy

Aliquots of aggregation reaction mixtures were taken at different time points and visualized by electron microscopy. A 3 μl sample was placed on a freshly glow-discharged carbon-coated grid, allowed to adsorb for 2 minutes, and washed with deionized water before staining with 2 μl of 1% uranyl acetate and blotting. Grids were imaged on a Tecnai T12 microscope (FEI Co., Hillsboro, Oregon) operating at 120kV and 30,000x magnification, and equipped with an UltraScan 1000 CCD camera (Gatan, Pleasanton, California) with post-column magnification of 1.4x.

Recombinant protein expression

The region encoding amino acids M1 to G115 of the αHtt-V_L 12.3 domain was amplified by PCR using plasmid DNA (pNES-VL12.3, a gift from Dane Wittrup) as template. The resulting amplicon was then inserted into a pET15b expression vector (Novagen), using NdeI and XhoI restriction sites at the 5′ and 3′ ends, respectively, generating an N-terminal His-tagged αHtt-V_L 12.3 domain construct. Following sequence verification, the V_L12.3–15b plasmid was transformed into *E. coli* Rosetta2 (DE3) cells (Novagen). Cultures were grown at 37° C, induced with 1 mM IPTG at OD_{600} of ~0.8, and further grown at 16°C for 18 h for protein production. Cells were harvested by centrifugation, resuspended in TBS buffer (25 mM Tris.HCl, 150 mM NaCl, 3 mM NaN_3, and pH 8.0) and lyzed by sonication. Protein was purified by metal-affinity chromatography on Ni^{2+}-derivatized HisTrap columns (GE Healthcare) using a linear (20 – 1000 mM) imidazole gradient for elution. Purified protein was digested with thrombin in TBS buffer for removal of the His tag (leaving a Gly-Ser-His sequence at the N-terminus of the V_L protein), followed by gel filtration on Superdex75 (GE Healthcare) in 20 mM sodium phosphate, 100 mM NaCl, and 3 mM NaN_3 (pH 6.0). Purified proteins were concentrated using centriprep concentrators (Millipore) up to ~10 mg/ml and the buffer was simultaneously exchanged to 20 mM sodium phosphate, 3 mM NaN_3, 90/10% H_2O/D_2O (pH 6.0). Structure of the purified protein was confirmed by mass spectrometry.

RESULTS

A variety of proteolytic cleavage events generating short polyQ-containing fragments of htt have been implicated in the HD disease mechanism (29), and the expression of expanded polyQ forms of such fragments, including one particular fragment, htt exon-1 (Fig. 1), has been widely shown to lead to aggregation and/or toxicity in cells and animals (30–35).

Exon-1 consists of three well-defined sequence elements: the 17 amino acid htt^{NT} segment, the polyQ segment, and the Pro-rich segment (Fig. 1). Since chemically synthesized peptides containing the first two elements, plus polyPro segments as short as P_6, exhibit aggregation properties very similar to those of full length exon-1 (B. Sahoo, D. Singer, T. Zuchner and R. Wetzel, Ms. in preparation), we have used such C-terminally truncated derivatives of htt exon1 to work out details of the aggregation mechanism (16–18, 36). Synthetic peptides studied in this paper are shown in Figure 1.

Compromising the htt^{NT} role via inhibition with htt^{NT} peptides

Recently we reported that peptides related to the htt^{NT} sequence can be effective, if transitory, inhibitors of the aggregation of polyQ-containing htt fragment peptides (18). Thus, while 6 μM of $htt^{NT}Q_{30}P_6K_2$ exhibits measureable aggregation within several hrs and is 50% aggregated by 18 hrs, the same concentration of peptide in the presence of a 1:1 ratio of htt^{NT} shows little aggregation after 18 hrs and requires ~ 80 hrs to reach 50% aggregation (Fig. 2A). Since we reckoned that the polyQ element of $htt^{NT}Q_{30}P_6K_2$ might be capable of aggregating by several mechanisms, we inquired as to the nature of the residual aggregation that occurs in the presence of the htt^{NT} inhibitor. Electron micrographs of the non-inhibited aggregation of $htt^{NT}Q_{30}P_6K_2$ show early formation of spherical oligomers (Fig. 3B, 0.25 hrs), followed by protofibrils (Fig. 3C, 2.5 hrs) and ultimately rough-edged fibrils (Fig. 3D, 144 hrs) (16). In contrast, in addition to the expected (18) mixed oligomer inhibition complexes, early amyloid-like aggregates are observed at 5.5 hrs when $htt^{NT}Q_{30}P_6K_2$ is incubated in the presence of the htt^{NT} (Fig. S1H), and larger aggregates observed at 8.0 hrs (Fig. 3E; Fig. S1 I-P) exhibit the characteristic broad ribbons that are normally seen in amyloid aggregates of simple polyQ (Fig. 3J); such aggregates are never observed in uninhibited reactions of $htt^{NT}Q_N$ peptides. EM images of the htt^{NT} inhibited reaction taken at subsequent times show aggregate morphologies more resembling the protofibrillar (Fig. 3F, 45 hrs) and fibrillar (Fig. 3G, 68 hrs) aggregates normally observed at earlier times in the non-inhibited aggregation of $htt^{NT}Q_{30}P_6K_2$ (Fig 3B,C). The progression of aggregate morphologies suggest that at early times in the htt^{NT} inhibited reaction, there is a window within which $htt^{NT}Q_{30}P_6K_2$ peptides can nucleate amyloid growth *via* the pathway normally observed for simple polyQ peptides, leading to characteristic ribbon-like aggregates. Eventually, however, inhibition of htt^{NT}-mediated amyloid nucleation is overcome, and the characteristic aggregate morphologies observed in htt N-terminal peptide aggregation emerge.

Further kinetics studies add additional support to this view. An examination of the concentration dependence of the initial aggregation rates (Fig. 4) of wild type $htt^{NT}Q_{30}P_6K_2$ (■) and its F17W mutant (▲) in the absence of htt^{NT} inhibition yields log-log slopes of 1.20 and 0.95 as previously reported (16). In contrast, the corresponding slope for the same peptide in the presence of inhibitor (△) is 2.65, which is very similar to the slope of 2.57 for aggregation of a simple $K_2Q_{30}K_2$ peptide (●) (Fig. 4). This slope change is consistent with the EM data in suggesting that the early aggregation of $htt^{NT}Q_{30}P_6K_2$ in the presence of htt^{NT} occurs *via* the classical, nucleated growth mechanism previously determined for simple polyQ peptides (14, 15).

As a further test, the mature aggregates from the inhibited and non-inhibited aggregation reactions of $htt^{NT}Q_{30}P_6K_2$, along with control amyloid-like aggregates of $K_2Q_{30}K_2$, were collected and studied for their seeding properties, as a measure of structural relatedness (37, 38). With $htt^{NT}Q_{30}P_6K_2$ monomers, only the product from the non-inhibited aggregation of $htt^{NT}Q_{30}P_6K_2$ (●) exhibited significant enhancement compared with the non-seeded control (○), while $K_2Q_{30}K_2$ aggregates (△) and the products of htt^{NT}-inhibited $htt^{NT}Q_{30}P_6K_2$ aggregation (▲) were equally ineffective (Fig. 2B). With $K_2Q_{30}K_2$ monomers, the product of htt^{NT}-inhibited aggregation of $htt^{NT}Q_{30}P_6K_2$ (▲) likewise behaved like simple $K_2Q_{30}K_2$

aggregates (△), with both aggregates significantly enhancing aggregation compared to the unseeded control (○) (Fig. 2C). In contrast, the product of non-inhibited $htt^{NT}Q_{30}P_6K_2$ aggregation (●) was an ineffective seed, producing no change from the unseeded rate (Fig. 2C). Together the results show that (a) the seeding properties of non-inhibited $htt^{NT}Q_{30}P_6K_2$ aggregation and $K_2Q_{30}K_2$ aggregation are different, and (b) the seeding potential of the product of inhibited aggregation of $htt^{NT}Q_{30}P_6K_2$ is identical to that of $K_2Q_{30}K_2$ aggregates. These seeding results imply underlying structural similarities and differences. It is interesting that the final aggregates of the htt^{NT}-inhibited reaction behave like $K_2Q_{30}K_2$ aggregates, even though they are quite similar in appearance to the aggregates from the non-inhibited $htt^{NT}Q_{30}P_6K_2$ reaction (Fig. 3D,G). This shows that aggregate properties cannot always be correlated with EM morphologies.

Compromising the htt^{NT} role via inhibition with an anti-htt^{NT} intrabody

Previously, Wittrup and colleagues described a novel immunoglobulin-related molecule capable of binding the htt^{NT} segment of htt, obtained by a combination of mutagenesis and yeast surface display selection (39). This light chain variable domain-related protein, αHtt-V_L 12.3, which lacks both a heavy chain partner and the normal, native Ig fold intra-domain disulfide bond, exhibited a binding constant for htt^{NT} peptides in the low nM range (39, 40), inhibited htt N-terminal fragment aggregation *in vitro*, and was a good inhibitor of htt aggregation and toxicity in mammalian cells in culture (39). Interestingly, the X-ray crystal structure of a 1:1 complex of this VL 12.3 with an htt^{NT} fragment shows that htt^{NT} is bound in an α-helical conformation (40), similar to the structure induced upon htt^{NT} self-assembly into tetramers and larger oligomers (36) (17). We used a cDNA encoding this protein to engineer a vector for expression in E. coli (see Methods). After purification and proteolytic removal of the His tag, the 12 kDa protein was obtained and examined for its mechanism of aggregation inhibition.

In our standard sedimentation aggregation assay, this protein proved a very effective inhibitor of $htt^{NT}Q_{30}P_6K_2$ aggregation at a 1:1 molar ratio (Fig. 5A). After a slow drop in soluble $htt^{NT}Q_{30}P_6K_2$ in the inhibited reaction to about 70% the starting value, little or no further loss of monomer occurs up to over 150 hrs (Fig. 5A, -○-). A small but significant amount of the αHtt-V_L 12.3 domain protein also becomes pelletable over the same time frame (Fig. 5A, -△-). In parallel with the generation of pelletable material, right angle light scattering confirmed the generation of protein particles (Fig. 5B). At the same time, there is no detectible ThT signal throughout the incubation of $htt^{NT}Q_{30}P_6K_2$ with the αHtt-V_L 12.3 domain protein (Fig. 5C), suggesting that the aggregates formed are not amyloid. Thus, in contrast to the inhibition by 1:1 ratios of htt^{NT} peptides, the αHtt-V_L 12.3 domain protein under the same conditions provides strong inhibition of htt^{NT}-mediated amyloid nucleation in polyQ-containing htt fragments. We conducted further experiments to explore this difference.

We first examined complex formation under native conditions between VL 12.3 and $htt^{NT}Q_{30}P_6K_2$, using SEC. As previously described (40), we found that the αHtt-V_L 12.3 domain protein behaves aberrantly in SEC, eluting well after the position normally occupied by small solute molecules (Fig. 6A, peak c). In contrast, the $htt^{NT}Q_{30}P_6K_2$ peptide elutes at 31.6 mins (Fig. 6A), corresponding to a predicted MW of 7.7 KDa. The slight discrepancy between the SEC determined MW and the actual (6.7 KDa) is most likely due to the non-globular nature of the htt N-terminal fragment (SEC standards used are all globular proteins; see Methods). A mixture of excess αHtt-V_L 12.3 domain protein with $htt^{NT}Q_{30}P_6K_2$ generates a new peak eluting at 29.2 mins (Fig. 6A, peak b), corresponding to an SEC determined MW of 12.6 KDa. This is somewhat lower than expected (19.0 kDa) for a 1:1 complex, perhaps due to some residual interaction of the αHtt-V_L 12.3 domain component with the solid support. Interestingly, the SEC profile of the mixture also exhibits several

higher MW forms, including a small peak corresponding to ~ 43 kDa (Fig. 6A). The main 29.2 min SEC peak was collected and analyzed by LC-MS (see Methods). In the RP-HPLC of this SEC peak, two peaks were observed, giving MS signals corresponding to the known masses of $htt^{NT}Q_{30}P_6K_2$ and the αHtt-V_L 12.3 domain protein (Fig. 6B). Thus, the major product of the initial interaction of $htt^{NT}Q_{30}P_6K_2$ and the αHtt-V_L 12.3 domain protein in solution is, as expected from other analyses (40), a 1:1 complex.

Further examination of the incubated mixture of these two proteins by EM revealed additional higher assembly forms. EM images collected at 120 hrs consistently show a field of spherical aggregates with aggregates in the 8 –25 nm range (Fig. 3H). There is a curious 'beads-on-a-string' appearance to these images, the significance of which is not clear. These large oligomers presumably are the source of the ThT-negative (Fig. 5C), light scattering positive (Fig. 5B) material as well as the incomplete recovery of monomer in the sedimentation assay from solutions of $htt^{NT}Q_{30}P_6K_2$ and the αHtt-V_L 12.3 domain protein (Fig. 5A). It is tempting to assign the observed strong inhibition of amyloid formation to the existence of these oligomers, in analogy to other peptide-based inhibitors of the aggregation of polyQ-containing htt fragments (18). This interpretation does not hold up under scrutiny, however. Since oligomer formation does not nearly go to completion (Fig. 5A), it would be expected that the residual (~70%) concentration of low MW material should be capable of supporting the alternative amyloid formation pathway, as in the case of htt^{NT} inhibition described above. There is no evidence of this, however, by EM or other analysis. Based on the SEC analysis (Fig. 6A), it is likely that the bulk of the $htt^{NT}Q_{30}P_6K_2$ in this solution is engaged in complex formation with the V_L 12.3 protein to generate a heterodimer (Fig. 6A). It would therefore appear that this heterodimer formation is sufficient to very effectively block nucleation of polyQ amyloid formation. This suggests an ability of the 1:1 complex to interfere with the interactions of the polyQ chains that are required to engage the classical nucleated growth mechanism seen for simple polyQ peptides and for htt^{NT}-inhibited $htt^{NT}Q_{30}P_6K_2$ (see above). It is not clear how complexation of the V_L protein with the htt^{NT} segment alone might achieve this.

Compromising the htt^{NT} role via partial excission

Previously we showed that the polyQ containing fragment of trypsin cleavage of $htt^{NT}Q_{37}P_{10}K_2$, namely, SF-$Q_{37}P_{10}K_2$, undergoes amyloid nucleation at a slower rate than the uncleaved molecule, and exhibits a nucleation mechanism and aggregate morphologies identical to those from simple polyQ peptides (15). Consistent with the suggestion that similar cleavage fragments occur in cells (41), tg mouse experiments have been initiated investigating the effect of expression of a full length htt molecule in which the 17 amino acid htt^{NT} sequence is replaced by the Met-Phe sequence (William Yang, personal communication). Here we investigate the impact of this sequence change in aggregation experiments *in vitro*.

As expected, the peptide MF-$Q_{37}P_{10}K_2$ (○) aggregates appreciably more slowly than a matched concentration of $htt^{NT}Q_{37}P_{10}K_2$ (●) (Fig. 7A). At the same time, however, M*F*-$Q_{37}P_{10}K_2$ at a higher concentration (●) aggregates somewhat faster than the same concentration of $Q_{37}P_{10}K_2$ (◇) (Fig. 7B). Analysis of the concentration dependence of the initial aggregation of MF-$Q_{37}P_{10}K_2$ yields a log-log plot (Fig. 4, ◇) slope of 2.5, almost identical to the slopes for $K_2Q_{30}K_2$ (●) and the htt^{NT}-inhibited aggregation of $htt^{NT}Q_{30}P_6K_2$ (△). Finally, the morphology of the MF-$Q_{37}P_{10}K_2$ aggregates (Fig. 3I) is identical to typical amyloid-like aggregates of simple polyQ peptides (Fig. 3J). Thus, aggregation kinetics and aggregate morphologies are consistent in indicating that this analog of a trypsin-cleaved htt N-terminal fragment follows an aggregation pathway essentially identical to that of simple polyQ peptides.

DISCUSSION

The phenomenon of aggregate polymorphism has emerged as a major area of interest in amyloid assembly and properties (11, 42, 43). The ability to make multiple morphologies of stable products is nearly ubiquitous in amyloid systems and distinguishes them from native proteins. For example, not only do amyloidogenic peptides like Aβ exhibit a variety of aggregate non-amyloid morphologies, some of which may be particularly toxic (44), but even mature amyloid fibrils of the same wild type Aβ peptide can exhibit a surprising number of distinct structural types (45–47). The polymorphisms exhibited by mature amyloid fibrils are almost certainly linked to the phenomena of strain effects in prion biology, at least in yeast prion systems (11, 43). While the ability of protein aggregates to exhibit multiple, stable structural types is accounted for by the polymeric nature of protein assemblies (48), the mechanistic basis for how growth conditions (6, 19, 49–51), mutations (7, 52–54), and/or other, sporadic, factors (55) control the kinetic accessibility that ultimately favors particular aggregate polymorphs has received less attention. This general problem may be particularly well-defined in the huntingtin system. While simple polyQ peptides are almost unique in the amyloid world in being able to assemble into amyloid fibrils without the mediation of non-amyloid intermediates (15), certain flanking sequences to polyQ, such as the htt^{NT} segment of huntingtin (16, 17), mediate amyloid nucleation by undergoing an initial, independent assembly pathway (2). At the same time, in contrast to the current wisdom that such oligomers tend to be the primary toxic agents in aggregation-based neurodegenerative diseases (42), the situation may be different in polyQ diseases. We have argued that the reported low toxicity (24) of a htt exon1 analog containing a particular type of proline-mutated polyQ segment (56) is evidence against a toxic role for non-amyloid oligomers of htt fragments (18). Consistent with this view, a well-supported mechanism for aggregate toxicity in polyQ diseases, the recruitment/sequestration hypothesis (22), is only likely to operate *via* mature amyloid-like polyQ aggregates, and not with oligomers, due to the relative abilities of these two aggregate classes to seed aggregate elongation (16) and hence recruit monomers. Perhaps related to such functional diversity, different morphologies of polyQ aggregates have been shown to exhibit different cytotoxicities (19).

Our working model for the aggregation options open to polyQ-containing htt fragments is shown in Figure 8. Monomers (a) of such fragments are in principle capable of entering two distinct aggregation pathways. Pathway A involves the efficient formation of α-helix rich oligomers according to the pathway described previously (16, 17). In this pathway, the htt^{NT} segment of these peptides, which is disordered in the monomer state (16), mediates α-helix bundle formation (b,c,d) that collects the disordered polyQ elements at a high local concentration and thereby facilitates the formation of polyQ amyloid nuclei (e) that can then elongate into βrich amyloid like aggregates by monomer addition (f). (It should be noted that alternative models have also been described for how flanking sequences interact with polyQ sequences to effect aggregate formation (57–59)). If, for any of a number of reasons, htt^{NT} mediated α-helix bundle formation is not feasible or efficient, polyQ-containing htt fragments can undergo the previously described (14, 15) classical nucleation pathway. In this B Pathway, for relatively long (15) polyQ peptides, the critical nucleus is a special, rare conformation of the monomer (g) that is capable of serving as the template for the initiation of amyloid elongation (h). This paper concerns cases in which the role of the htt^{NT} sequence is compromised by virtue of its removal, or by the action of certain htt^{NT}-complexation agents. Elsewhere we will describe what happens when htt^{NT} function is compromised due to sequence modifications within htt^{NT}, such as post-translational modifications (52) (R. Mishra and R. Wetzel, manuscripts in preparation).

As previously described (18), htt^{NT} and related sequences appear to inhibit pathway A by readily forming mixed α-helical oligomers with the polyQ-containing htt N-terminal

fragment. This dilutes the local concentration of the disordered polyQ segments and hence retards nucleation. At the same time, inhibition is incomplete, so that nucleation and growth of amyloid do finally occur (18). As we shown here, when pathway A is transiently restricted, pathway B remains open, resulting in a concentration dependence characteristic of the B (and not the A) pathway, and in the formation of polyQ amyloid aggregates that resemble aggregates of simple polyQ peptides both in the EM (Fig. 3E; Fig. S1, I-P) and in their cross-seeding properties (Fig. 2B,C). These data show that the lack of evidence for the simple polyQ aggregation pathway in $htt^{NT}Q_N$ peptides under most circumstances is not because this pathway is inactivated by the htt^{NT} moiety, but rather because it is outstripped kinetically by the alternate, htt^{NT}-mediated pathway. When the kinetic advantage of the htt^{NT}-mediated pathway is compromised, the simple polyQ nucleation and aggregation pathway effectively competes. The kinetic partitioning between these two well-characterized pathways of amyloid nucleation and growth provides a molecular basis for how certain chaperones can influence the course of huntingtin fragment aggregation (57, 60, 61). In Figure 8, the products of pathway B are drawn to indicate the absence of the fully formed htt^{NT} α-helix that is known to exist in the final product of pathway A (17, 36). The fate of the htt^{NT} segment in these aggregates is unknown, however, and the altered structure is indicated schematically only as a reminder that the final aggregates must be structurally different at some level, since they are functionally different. In fact, the basis for the difference in seeding abilities of the final aggregates of the inhibited and non-inhibited reactions is not clear. This may be a consequence of the amount of htt^{NT} inhibitor that appears to be bound to the fibrils (18). Alternatively, it may reflect some very subtle structural difference of the polyQ β-sheet networks of these two fibrils.

Although the V_L 12.3 protein also likely inhibits pathway A by specifically complexing htt^{NT} and preventing its self-association, there is no evidence for the formation of pathway B products, in contrast to the results of htt^{NT} inhibition. Our data suggest that, even after long incubation, the bulk of a mixture of V_L 12.3 and htt N-terminal fragment consists of heterodimers of these two proteins, with only a minor portion of the proteins involved in the formation of large oligomers. It might have been expected that the polyQ segment of $htt^{NT}Q_{30}P_6K_2$ in these heterodimers might be as free to engage the B pathway (Fig. 8) as are $htt^{NT}Q_{30}P_6K_2$ monomers under htt^{NT} inhibition, but there is no evidence that this pathway is open to the V_L 12.3/$htt^{NT}Q_N$ heterodimers. This implies that, in spite of the focus of V_L 12.3 on the htt^{NT} segment, the polyQ sequence in the heterodimer exists in a conformational state that resists the nucleation and/or elongation steps shown in the B pathway.

Since we previously showed that polyQ peptides containing a C-terminal polyPro extension undergo amyloid nucleation by the same mechanism as simple polyQ peptides (62), it is not surprising that the peptide MF-$Q_{37}P_{10}K_2$ exhibits a log-log slope similar to that of $K_2Q_{30}K_2$ (Fig. 4). The more rapid aggregation in the 40 μM range of MF-$Q_{37}P_{10}K_2$ compared with $Q_{37}P_{10}K_2$, however, shows that the MF sequence does play a role in aggregation. Just as the Ser-Phe sequence of htt^{NT} proximal to the polyQ has been shown to take part in β-sheet formation in the mature amyloid fibrils of htt N-terminal fragments (36), it is possible that the polyQ proximal Met-Phe in MF-$Q_{37}P_{10}K_2$ is included in amyloid structure and by virtue of that might affect nucleation or elongation in a positive way. Regardless of this slight enhancing effect, however, it is also clear that MF-$Q_{37}P_{10}K_2$ aggregates much less rapidly than the corresponding $htt^{NT}Q_{37}P_{10}K_2$ (Fig. 7A), and this rate difference is expected to be greatly enhanced at the low concentrations that obtain in the cell, based on a projection to low, cellular concentrations from their disparate concentration dependencies (Fig. 4).

Although the htt^{NT} segment of htt has a number of important possible targeting and trafficking roles (63–67), it is clear from these and other studies (16–18, 36, 52, 57) that this flanking sequence of the polyQ also greatly contributes to biophysical properties. The data

presented in this paper show that different fates of the htt^{NT} segment of polyQ-containing htt fragments can have different consequences, not only for aggregation rates, but also for the mechanism of aggregation and hence for the structure and properties of the aggregate products. Thus, htt^{NT} inhibition of $htt^{NT}Q_N$ aggregation produces amyloid aggregates that are much more capable of recruiting other polyQ proteins into the growing aggregate than are the amyloid products of non-inhibited aggregation reactions (Fig. 2C). This observation is relevant to the recent description of the seeding ability of aggregates isolated from various HD tg mice (20), and to recruitment-sequestration models of polyQ toxicity (21, 22). It remains to be seen whether there exist molecules in the cell capable of producing htt^{NT}-like inhibitory effects, but certain molecular chaperones are attractive candidates for such molecules (57, 60, 61). In contrast to htt^{NT}, the V_L 12.3 protein completely blocks amyloid formation *in vitro*, instead generating a mixture of heterodimers and non-amyloid oligomers. Given this result, the observation that this protein in cell culture inhibits both inclusion formation and cytotoxicity (68) is most consistent with the hypothesis, discussed above, that it is the amyloid fibril form of polyQ-containing htt fragments that are toxic, while non-amyloid oligomers are benign (18). Given that the removal of the htt^{NT} segment from htt N-terminal fragments slows but does not abrogate polyQ amyloid formation, while completely eliminating the ability of such fragments to make non-amyloid oligomers, it will be interesting to consider the effects of this modification on disease course and neuronal pathology observed in ongoing tg mouse experiments (Gu et al., Ms. in preparation).

Supplementary Material

Refer to Web version on PubMed Central for supplementary material.

Acknowledgments

Funding support from the National Institutes of Health, R01 AG019322 (to R.W.) and SAP #4100026429 from the Commonwealth of Pennsylvania (to A.M.G.).

We gratefully acknowledge Dane Wittrup (MIT) for the gift of the cDNA encoding the αHtt-V_L 12.3 domain protein, and discussions with William Yang (UCLA). We thank Bart Roland for providing some of the aggregation kinetics data, and Drs. James Conway and Alexander Makhov for helpful discussions and access to the Structural Biology Department's cryo-EM facility.

ABBREVIATIONS AND TEXTUAL FOOTNOTES

polyQ	polyglutamine
htt	huntingtin
htt^{NT}	17 amino acid N-terminus of huntingtin preceding the polyQ sequence
anti-htt^{NT} V_L 12.3 protein	immunoglobulin light chain variable domain-derived htt^{NT} binding protein
HD	Huntington's disease

References

1. Bates, GP.; Benn, C. The polyglutamine diseases. In: Bates, GP.; Harper, PS.; Jones, L., editors. Huntington's Disease. Oxford University Press; Oxford, U.K: 2002. p. 429-472.
2. Wetzel R. Physical chemistry of polyglutamine: Intriguing tales of a monotonous sequence. J Mol Biol. 2012 in press. 10.1016/j.jmb.2012.01.030
3. Scherzinger E, Sittler A, Schweiger K, Heiser V, Lurz R, Hasenbank R, Bates GP, Lehrach H, Wanker EE. Self-assembly of polyglutamine-containing huntingtin fragments into amyloid-like

fibrils: implications for Huntington's disease pathology. Proc Natl Acad Sci U S A. 1999; 96:4604–4609. [PubMed: 10200309]

4. Chen S, Berthelier V, Yang W, Wetzel R. Polyglutamine aggregation behavior *in vitro* supports a recruitment mechanism of cytotoxicity. J Mol Biol. 2001; 311:173–182. [PubMed: 11469866]
5. Wilburn B, Rudnicki DD, Zhao J, Weitz TM, Cheng Y, Gu XF, Greiner E, Park CS, Wang N, Sopher BL, La Spada AR, Osmand A, Margolis RL, Sun YE, Yang XW. An antisense CAG repeat transcript at JPH3 locus mediates expanded polyglutamine protein toxicity in Huntington's disease-like 2 mice. Neuron. 2011; 70:427–440. [PubMed: 21555070]
6. Wood SJ, Maleeff B, Hart T, Wetzel R. Physical, morphological and functional differences between pH 5.8 and 7.4 aggregates of the Alzheimer's peptide Ab. J Mol Biol. 1996; 256:870–877. [PubMed: 8601838]
7. Helms LR, Wetzel R. Specificity of abnormal assembly in immunoglobulin light chain deposition disease and amyloidosis. J Mol Biol. 1996; 257:77–86. [PubMed: 8632461]
8. Kirkitadze MD, Bitan G, Teplow DB. Paradigm shifts in Alzheimer's disease and other neurodegenerative disorders: the emerging role of oligomeric assemblies. J Neurosci Res. 2002; 69:567–577. [PubMed: 12210822]
9. Caughey B, Lansbury PT. Protofibrils, pores, fibrils, and neurodegeneration: separating the responsible protein aggregates from the innocent bystanders. Annu Rev Neurosci. 2003; 26:267–298. [PubMed: 12704221]
10. Glabe CG, Kayed R. Common structure and toxic function of amyloid oligomers implies a common mechanism of pathogenesis. Neurology. 2006; 66:S74–78. [PubMed: 16432151]
11. Kodali R, Wetzel R. Polymorphism in the intermediates and products of amyloid assembly. Curr Opin Struct Biol. 2007; 17:48–57. [PubMed: 17251001]
12. Ross CA, Poirier MA. Opinion: What is the role of protein aggregation in neurodegeneration? Nat Rev Mol Cell Biol. 2005; 6:891–898. [PubMed: 16167052]
13. Sathasivam K, Lane A, Legleiter J, Warley A, Woodman B, Finkbeiner S, Paganetti P, Muchowski PJ, Wilson S, Bates GP. Identical oligomeric and fibrillar structures captured from the brains of R6/2 and knock-in mouse models of Huntington's disease. Hum Mol Genet. 2010; 19:65–78. [PubMed: 19825844]
14. Chen S, Ferrone F, Wetzel R. Huntington's Disease age-of-onset linked to polyglutamine aggregation nucleation. Proc Natl Acad Sci USA. 2002; 99:11884–11889. [PubMed: 12186976]
15. Kar K, Jayaraman M, Sahoo B, Kodali R, Wetzel R. Critical nucleus size for disease-related polyglutamine aggregation is repeat-length dependent. Nat Struct Mol Biol. 2011; 18:328–336. [PubMed: 21317897]
16. Thakur AK, Jayaraman M, Mishra R, Thakur M, Chellgren VM, Byeon IJ, Anjum DH, Kodali R, Creamer TP, Conway JF, Gronenborn AM, Wetzel R. Polyglutamine disruption of the huntingtin exon 1 N terminus triggers a complex aggregation mechanism. Nat Struct Mol Biol. 2009; 16:380–389. [PubMed: 19270701]
17. Jayaraman M, Kodali R, Sahoo B, Thakur AK, Mayasundari A, Mishra R, Peterson CB, Wetzel R. Slow amyloid nucleation via α-helix-rich oligomeric intermediates in short polyglutamine-containing Huntingtin fragments. J Mol Biol. 2012; 415:881–899. [PubMed: 22178474]
18. Mishra R, Jayaraman M, Roland BP, Landrum E, Fullam R, Kodali R, Thakur AK, Arduini I, Wetzel R. Inhibiting nucleation of amyloid structure in a huntingtin fragment by targeting α-helix rich oligomeric intermediates. J Mol Biol. 2012; 415:900–917. [PubMed: 22178478]
19. Nekooki-Machida Y, Kurosawa M, Nukina N, Ito K, Oda T, Tanaka M. Distinct conformations of in vitro and in vivo amyloids of huntingtin-exon1 show different cytotoxicity. Proc Natl Acad Sci U S A. 2009; 106:9679–9684. [PubMed: 19487684]
20. Gupta S, Jie S, Colby DW. Protein misfolding detected early in the pathogenesis of a transgenic mouse model of Huntington's disease using an amyloid seeding assay. J Biol Chem. 2011
21. Nucifora FC Jr, Sasaki M, Peters MF, Huang H, Cooper JK, Yamada M, Takahashi H, Tsuji S, Troncoso J, Dawson VL, Dawson TM, Ross CA. Interference by huntingtin and atrophin-1 with cbp-mediated transcription leading to cellular toxicity. Science. 2001; 291:2423–2428. [PubMed: 11264541]

22. McCampbell A, Fischbeck KH. Polyglutamine and CBP: fatal attraction? Nat Med. 2001; 7:528–530. [PubMed: 11329046]

23. Bucciantini M, Giannoni E, Chiti F, Baroni F, Formigli L, Zurdo J, Taddei N, Ramponi G, Dobson CM, Stefani M. Inherent toxicity of aggregates implies a common mechanism for protein misfolding diseases. Nature. 2002; 416:507–511. [PubMed: 11932737]

24. Poirier MA, Jiang H, Ross CA. A structure-based analysis of huntingtin mutant polyglutamine aggregation and toxicity: evidence for a compact beta-sheet structure. Hum Mol Genet. 2005; 14:765–774. [PubMed: 15689354]

25. Zhang QC, Yeh TL, Leyva A, Frank LG, Miller J, Kim YE, Langen R, Finkbeiner S, Amzel ML, Ross CA, Poirier MA. A compact beta model of huntingtin toxicity. J Biol Chem. 2011; 286:8188–8196. [PubMed: 21209075]

26. O'Nuallain B, Thakur AK, Williams AD, Bhattacharyya AM, Chen S, Thiagarajan G, Wetzel R. Kinetics and thermodynamics of amyloid assembly using a high-performance liquid chromatography-based sedimentation assay. Methods Enzymol. 2006; 413:34–74. [PubMed: 17046390]

27. Chen S, Berthelier V, Hamilton JB, O'Nuallain B, Wetzel R. Amyloid-like features of polyglutamine aggregates and their assembly kinetics. Biochemistry. 2002; 41:7391–7399. [PubMed: 12044172]

28. Jayaraman M, Thakur AK, Kar K, Kodali R, Wetzel R. Assays for studying nucleated aggregation of polyglutamine proteins. Methods. 2011; 53:246–254. [PubMed: 21232603]

29. Zuccato C, Valenza M, Cattaneo E. Molecular mechanisms and potential therapeutical targets in Huntington's disease. Physiol Rev. 2010; 90:905–981. [PubMed: 20664076]

30. Davies SW, Turmaine M, Cozens BA, DiFiglia M, Sharp AH, Ross CA, Scherzinger E, Wanker EE, Mangiarini L, Bates GP. Formation of neuronal intranuclear inclusions underlies the neurological dysfunction in mice transgenic for the HD mutation. Cell. 1997; 90:537–548. [PubMed: 9267033]

31. Faber PW, Alter JR, MacDonald ME, Hart AC. Polyglutamine-mediated dysfunction and apoptotic death of a Caenorhabditis elegans sensory neuron. Proc Natl Acad Sci U S A. 1999; 96:179–184. [PubMed: 9874792]

32. Krobitsch S, Lindquist S. Aggregation of huntingtin in yeast varies with the length of the polyglutamine expansion and the expression of chaperone proteins. Proc Natl Acad Sci U S A. 2000; 97:1589–1594. [PubMed: 10677504]

33. Apostol BL, Kazantsev A, Raffioni S, Illes K, Pallos J, Bodai L, Slepko N, Bear JE, Gertler FB, Hersch S, Housman DE, Marsh JL, Thompson LM. A cell-based assay for aggregation inhibitors as therapeutics of polyglutamine-repeat disease and validation in Drosophila. Proc Natl Acad Sci U S A. 2003; 100:5950–5955. [PubMed: 12730384]

34. Aiken CT, Tobin AJ, Schweitzer ES. A cell-based screen for drugs to treat Huntington's disease. Neurobiol Dis. 2004; 16:546–555. [PubMed: 15262266]

35. Wang CE, Tydlacka S, Orr AL, Yang SH, Graham RK, Hayden MR, Li S, Chan AW, Li XJ. Accumulation of N-terminal mutant huntingtin in mouse and monkey models implicated as a pathogenic mechanism in Huntington's disease. Hum Mol Genet. 2008; 17:2738–2751. [PubMed: 18558632]

36. Sivanandam VN, Jayaraman M, Hoop CL, Kodali R, Wetzel R, van der Wel PC. The aggregation-enhancing huntingtin N-terminus is helical in amyloid fibrils. J Am Chem Soc. 2011; 133:4558–4566. [PubMed: 21381744]

37. O'Nuallain B, Williams AD, Westermark P, Wetzel R. Seeding specificity in amyloid growth induced by heterologous fibrils. J Biol Chem. 2004; 279:17490–17499. [PubMed: 14752113]

38. Krebs MR, Morozova-Roche LA, Daniel K, Robinson CV, Dobson CM. Observation of sequence specificity in the seeding of protein amyloid fibrils. Protein Sci. 2004; 13:1933–1938. [PubMed: 15215533]

39. Colby DW, Garg P, Holden T, Chao G, Webster JM, Messer A, Ingram VM, Wittrup KD. Development of a human light chain variable domain (V(L)) intracellular antibody specific for the amino terminus of huntingtin via yeast surface display. J Mol Biol. 2004; 342:901–912. [PubMed: 15342245]

40. Schiefner A, Chatwell L, Korner J, Neumaier I, Colby DW, Volkmer R, Wittrup KD, Skerra A. A Disulfide-Free Single-Domain V(L) Intrabody with Blocking Activity towards Huntingtin Reveals a Novel Mode of Epitope Recognition. J Mol Biol. 2011; 414:337–355. [PubMed: 21968397]
41. Southwell AL, Bugg CW, Kaltenbach LS, Dunn D, Butland S, Weiss A, Paganetti P, Lo DC, Patterson PH. Perturbation with intrabodies reveals that calpain cleavage is required for degradation of huntingtin exon 1. PLoS ONE. 2011; 6:e16676. [PubMed: 21304966]
42. Stefani M. Structural polymorphism of amyloid oligomers and fibrils underlies different fibrillization pathways: immunogenicity and cytotoxicity. Curr Protein Pept Sci. 2010; 11:343–354. [PubMed: 20423295]
43. Toyama, BH.; Weissman, JS. Annual Review of Biochemistry. Vol. 80. Annual Reviews; Palo Alto: 2011. Amyloid Structure: Conformational Diversity and Consequences; p. 557-585.
44. Glabe CG. Structural classification of toxic amyloid oligomers. J Biol Chem. 2008; 283:29639–29643. [PubMed: 18723507]
45. Goldsbury CS, Wirtz S, Muller SA, Sunderji S, Wicki P, Aebi U, Frey P. Studies on the in vitro assembly of a beta 1–40: implications for the search for a beta fibril formation inhibitors. J Struct Biol. 2000; 130:217–231. [PubMed: 10940227]
46. Paravastua AK, Leapman RD, Yau WM, Tycko R. Molecular structural basis for polymorphism in Alzheimer's beta-amyloid fibrils. Proc Natl Acad Sci U S A. 2008; 105:18349–18354. [PubMed: 19015532]
47. Kodali R, Williams AD, Chemuru S, Wetzel R. A beta(1–40) Forms Five Distinct Amyloid Structures whose beta-Sheet Contents and Fibril Stabilities Are Correlated. Journal of Molecular Biology. 2010; 401:503–517. [PubMed: 20600131]
48. Wetzel R, Shivaprasad S, Williams AD. Plasticity of amyloid fibrils. Biochemistry. 2007; 46:1–10. [PubMed: 17198370]
49. Tanaka M, Chien P, Naber N, Cooke R, Weissman JS. Conformational variations in an infectious protein determine prion strain differences. Nature. 2004; 428:323–328. [PubMed: 15029196]
50. Kumar S, Udgaonkar JB. Conformational conversion may precede or follow aggregate elongation on alternative pathways of amyloid protofibril formation. J Mol Biol. 2009; 385:1266–1276. [PubMed: 19063899]
51. Kumar S, Udgaonkar JB. Structurally distinct amyloid protofibrils form on separate pathways of aggregation of a small protein. Biochemistry. 2009; 48:6441–6449. [PubMed: 19505087]
52. Gu X, Greiner ER, Mishra R, Kodali R, Osmand A, Finkbeiner S, Steffan JS, Thompson LM, Wetzel R, Yang XW. Serines 13 and 16 are critical determinants of full-length human mutant huntingtin induced disease pathogenesis in HD mice. Neuron. 2009; 64:828–840. [PubMed: 20064390]
53. Furukawa Y, Kaneko K, Yamanaka K, Nukina N. Mutation-dependent polymorphism of Cu,Zn-superoxide dismutase aggregates in the familial form of amyotrophic lateral sclerosis. J Biol Chem. 2010; 285:22221–22231. [PubMed: 20404329]
54. Ding F, Furukawa Y, Nukina N, Dokholyan NV. Local Unfolding of Cu, Zn Superoxide Dismutase Monomer Determines the Morphology of Fibrillar Aggregates. J Mol Biol. 2011
55. Goldsbury C, Frey P, Olivieri V, Aebi U, Muller SA. Multiple assembly pathways underlie amyloid-beta fibril polymorphisms. J Mol Biol. 2005; 352:282–298. [PubMed: 16095615]
56. Thakur A, Wetzel R. Mutational analysis of the structural organization of polyglutamine aggregates. Proc Natl Acad Sci U S A. 2002; 99:17014–17019. [PubMed: 12444250]
57. Tam S, Spiess C, Auyeung W, Joachimiak L, Chen B, Poirier MA, Frydman J. The chaperonin TRiC blocks a huntingtin sequence element that promotes the conformational switch to aggregation. Nat Struct Mol Biol. 2009; 16:1279–1285. [PubMed: 19915590]
58. Williamson TE, Vitalis A, Crick SL, Pappu RV. Modulation of polyglutamine conformations and dimer formation by the N-terminus of huntingtin. J Mol Biol. 2010; 396:1295–1309. [PubMed: 20026071]
59. Fiumara F, Fioriti L, Kandel ER, Hendrickson WA. Essential role of coiled coils for aggregation and activity of Q/N-rich prions and PolyQ proteins. Cell. 2010; 143:1121–1135. [PubMed: 21183075]

60. Wacker JL, Zareie MH, Fong H, Sarikaya M, Muchowski PJ. Hsp70 and Hsp40 attenuate formation of spherical and annular polyglutamine oligomers by partitioning monomer. Nat Struct Mol Biol. 2004; 11:1215–1222. [PubMed: 15543156]

61. Tam S, Geller R, Spiess C, Frydman J. The chaperonin TRiC controls polyglutamine aggregation and toxicity through subunit-specific interactions. Nat Cell Biol. 2006; 8:1155–1162. [PubMed: 16980959]

62. Bhattacharyya A, Thakur AK, Chellgren VM, Thiagarajan G, Williams AD, Chellgren BW, Creamer TP, Wetzel R. Oligoproline effects on polyglutamine conformation and aggregation. J Mol Biol. 2006; 355:524–535. [PubMed: 16321399]

63. Steffan JS, Agrawal N, Pallos J, Rockabrand E, Trotman LC, Slepko N, Illes K, Lukacsovich T, Zhu YZ, Cattaneo E, Pandolfi PP, Thompson LM, Marsh JL. SUMO modification of Huntingtin and Huntington's disease pathology. Science. 2004; 304:100–104. [PubMed: 15064418]

64. Atwal RS, Xia J, Pinchev D, Taylor J, Epand RM, Truant R. Huntingtin has a membrane association signal that can modulate huntingtin aggregation, nuclear entry and toxicity. Hum Mol Genet. 2007; 16:2600–2615. [PubMed: 17704510]

65. Rockabrand E, Slepko N, Pantalone A, Nukala VN, Kazantsev A, Marsh JL, Sullivan PG, Steffan JS, Sensi SL, Thompson LM. The first 17 amino acids of Huntingtin modulate its sub-cellular localization, aggregation and effects on calcium homeostasis. Hum Mol Genet. 2007; 16:61–77. [PubMed: 17135277]

66. Thompson LM, Aiken CT, Kaltenbach LS, Agrawal N, Illes K, Khoshnan A, Martinez-Vincente M, Arrasate M, JGOS-R, Khashwji H, Lukacsovich T, Zhu YZ, Lau AL, Massey A, Hayden MR, Zeitlin SO, Finkbeiner S, Green KN, Laferla FM, Bates G, Huang L, Patterson PH, Lo DC, Cuervo AM, Marsh JL, Steffan JS. IKK phosphorylates Huntingtin and targets it for degradation by the proteasome and lysosome. J Cell Biol. 2009; 187:1083–1099. [PubMed: 20026656]

67. Atwal RS, Desmond CR, Caron N, Maiuri T, Xia JR, Sipione S, Truant R. Kinase inhibitors modulate huntingtin cell localization and toxicity. Nat Chem Biol. 2011; 7:453–460. [PubMed: 21623356]

68. Colby DW, Chu Y, Cassady JP, Duennwald M, Zazulak H, Webster JM, Messer A, Lindquist S, Ingram VM, Wittrup KD. Potent inhibition of huntingtin aggregation and cytotoxicity by a disulfide bond-free single-domain intracellular antibody. Proc Natl Acad Sci U S A. 2004; 101:17616–17621. [PubMed: 15598740]

Peptide Name	Amino Acid Sequence
Htt exon 1	MATLEKLMKA FESLKSF--- QQQQQQQQQQ QQQQQQQQQQ QQQ------- ---------- PPPPPPPPPP-Htt_C[a]
htt^{NT}	MATLEKLMKA FESLKSF
$htt^{NT}Q_{30}P_6K_2$	MATLEKLMKA FESLKSF--- QQQQQQQQQQ QQQQQQQQQQ QQQQQQQQQQ ---------- PPPPPP---- KK
$htt^{NT}Q_{30}P_6K_2$ (F17W)	MATLEKLMKA FESLKSW--- QQQQQQQQQQ QQQQQQQQQQ QQQQQQQQQQ ---------- PPPPPP---- KK
$htt^{NT}Q_{37}P_{10}K_2$	MATLEKLMKA FESLKSF--- QQQQQQQQQQ QQQQQQQQQQ QQQQQQQQQQ QQQQQQQ--- PPPPPPPPPP KK
$Q_{37}P_{10}K_2$	QQQQQQQQQQ QQQQQQQQQQ QQQQQQQQQQ QQQQQQQ--- PPPPPPPPPP KK
MF-$Q_{37}P_{10}K_2$	M--------- ------F--- QQQQQQQQQQ QQQQQQQQQQ QQQQQQQQQQ QQQQQQQ--- PPPPPPPPPP KK
$K_2Q_{30}K_2$	KK QQQQQQQQQQ QQQQQQQQQQ QQQQQQQQQQ KK

[a]Htt_C = PQLPQPPPQA QPLLPQPQPP PPPPPPPPGP AVAEEPPLHR P

Figure 1.
Sequences of the exon1 N-terminal fragment of huntingtin and the various synthetic peptides studied.

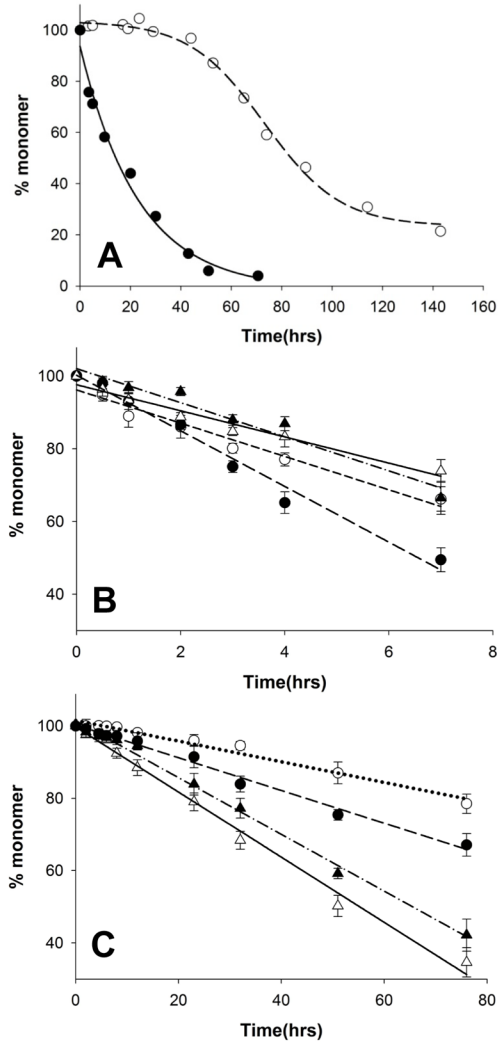

Figure 2.

Aspects of htt^{NT} inhibition. (A) Kinetics of $htt^{NT}Q_{30}P_6K_2$ with (○) and without (●) htt^{NT} inhibition. (B) Aggregation of approximately 4 μM $htt^{NT}Q_{30}P_6K_2$ either with no addition (○) or seeded with 7.5% by weight of: $K_2Q_{30}K_2$ fibrils (△); fibrils from $htt^{NT}Q_{30}P_6K_2$ aggregation with (▲) and without (●) added htt^{NT} inhibitor. (C) Aggregation of approximately 20 μM $K_2Q_{30}K_2$ either with no addition (○) or seeded with 5 % by weight of: $K_2Q_{30}K_2$ fibrils (△); fibrils from $htt^{NT}Q_{30}P_6K_2$ aggregation with (▲) and without (●) added htt^{NT} inhibitor. For comparison purposes, all data were fit to straight lines; linear fits are expected for efficient seeded elongation reactions (37), but not for the spontaneous, unseeded reactions (14–16). In fact, some deviation from linearity is seen in data from both of the non-seeded reactions.

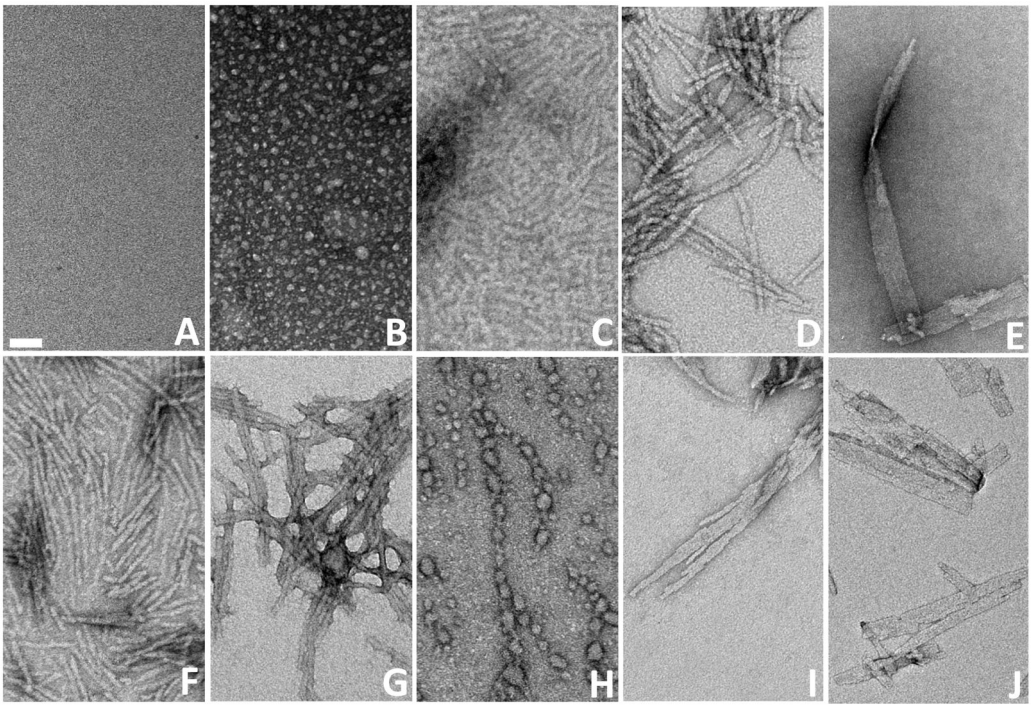

Figure 3.

Electron micrographs of various polyglutamine aggregates. Empty grid (A); aggregation reaction of $htt^{NT}Q_{30}P_6K_2$ alone at 15 mins (B), 2.5 hrs (C), and 100 hrs (D); aggregation of $htt^{NT}Q_{30}P_6K_2$ in the presence of a 1:1 molar ratio of htt^{NT} collected at 8 hrs (E), 45 hrs (F) and 68 hrs (G); aggregation of $htt^{NT}Q_{30}P_6K_2$ plus a 1:1 molar ratio of the anti-htt^{NT} V_L protein collected at 120 hrs (H); aggregation of MF-$Q_{37}P_{10}K_2$, 74 hrs (I); final aggregates of $K_2Q_{30}K_2$ (J). The scale bar (A) of 50 nm is applicable to all panels.

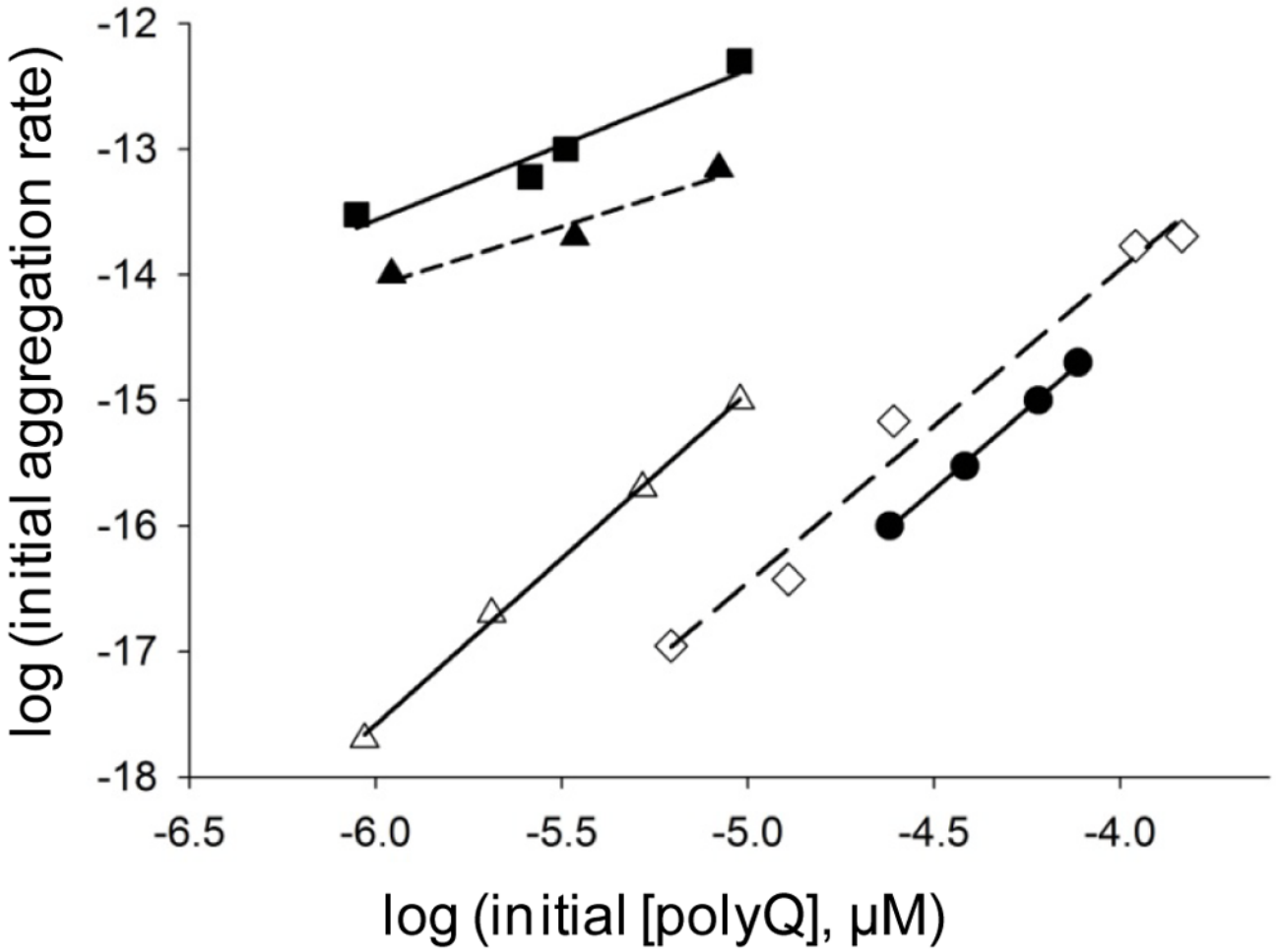

Figure 4.

Concentration dependence of initial aggregation rates of polyQ peptides. Slopes of time-squared plots of initial aggregation kinetic data are plotted vs. concentration in a log-log plot (14). The slope of the log-log plot minus 2 is n*, the critical nucleus (14). Determination for $K_2Q_{30}K_2$ (●, slope = 2.57, n* = 0.57), $htt^{NT}Q_{30}P_6$ (■, slope = 1.20, n* = − 0.80), $htt^{NT}Q_{30}P_6K_2$ (F17W) (▲, slope = 0.95, n* = − 1.05), $htt^{NT}Q_{30}P_6K_2$ (F17W) in the presence of htt^{NT} (△, slope = 2.65, n* = 0.65), and MF-$Q_{37}P_{10}K_2$ (◇, slope = 2.57, n* = 0.57). Previously we found that the F17W mutation (Methods) has a negligible effect on aggregation kinetics (16). Data for $K_2Q_{30}K_2$ and $htt^{NT}Q_{30}P_6K_2$ peptides alone are from reference (16).

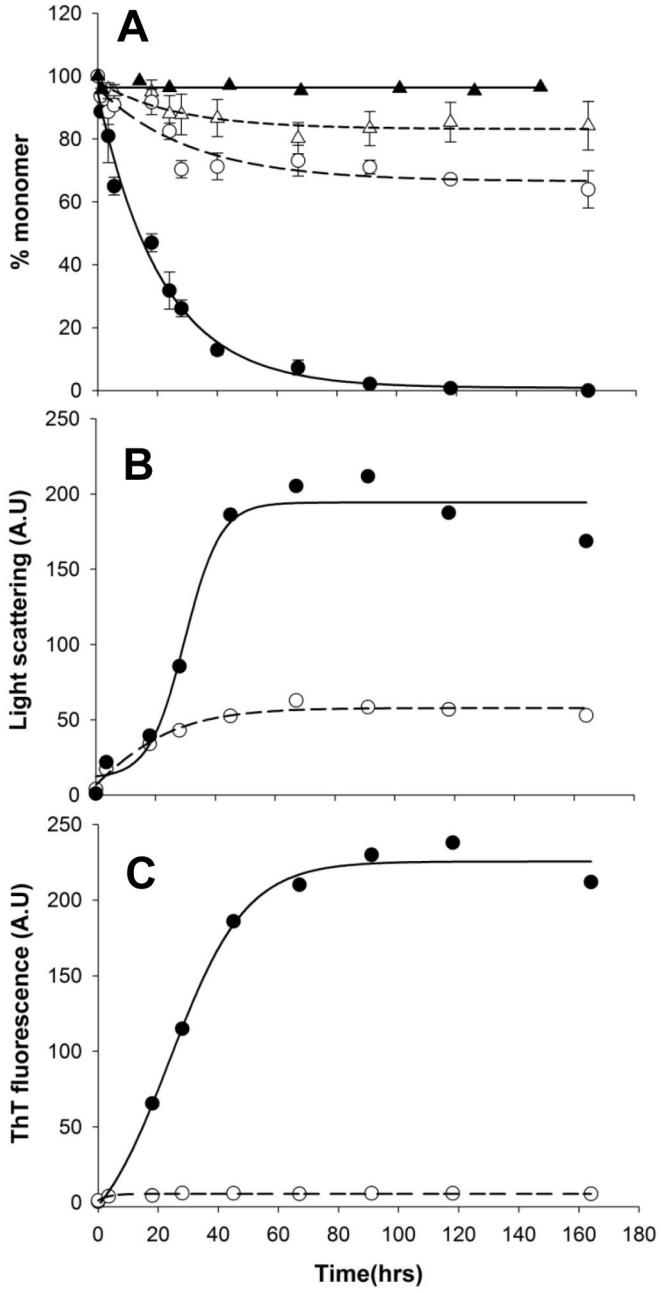

Figure 5.

Kinetics of aggregation of a 1:1 molar ratio of V_L 12.3 and $htt^{NT}Q_{30}P_6K_2$ by the sedimentation (A), 90° light scattering (B) and ThT (C) assays. $Htt^{NT}Q_{30}P_6K_2$ with (○) and without (●) the V_L protein; V_L protein monomer concentration in mixture with $htt^{NT}Q_{30}P_6K_2$ (△); V_L protein incubated alone (▲).

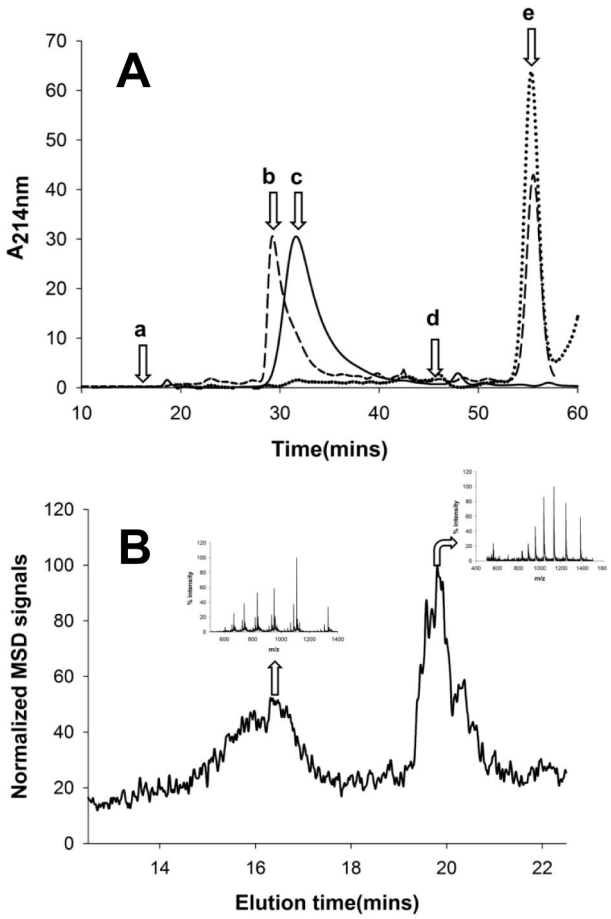

Figure 6.

Size exclusion chromatography of the anti-htt^{NT} V_L 12.3 protein. (A) Chromatograms of anti-htt^{NT} V_L 12.3 protein alone (dotted line), htt$^{NT}Q_{30}P_6K_2$ alone (solid line) and a mixture of htt$^{NT}Q_{30}P_6K_2$ with excess anti-htt^{NT} V_L 12.3 protein (dashed line). Arrows indicate void volume (a), htt$^{NT}Q_{30}P_6K_2$: anti-htt^{NT} V_L 12.3 complex (b, 29.2 mins, 12.6 KDa from standard curve; 19.0 KDa actual), htt$^{NT}Q_{30}P_6K_2$ alone (c, 31.6 mins, 7.7 KDa from standard curve, 6.7 KDa actual), position of salt elution (d), anti-htt^{NT} V_L 12.3 protein alone (e); (B) LC-MS of the SEC peak “b” above identifying two components with the m/z of htt$^{NT}Q_{30}P_6K_2$ eluting at ~ 16.5 mins and for the anti-htt^{NT} V_L 12.3 protein eluting at ~ 19.5 mins.

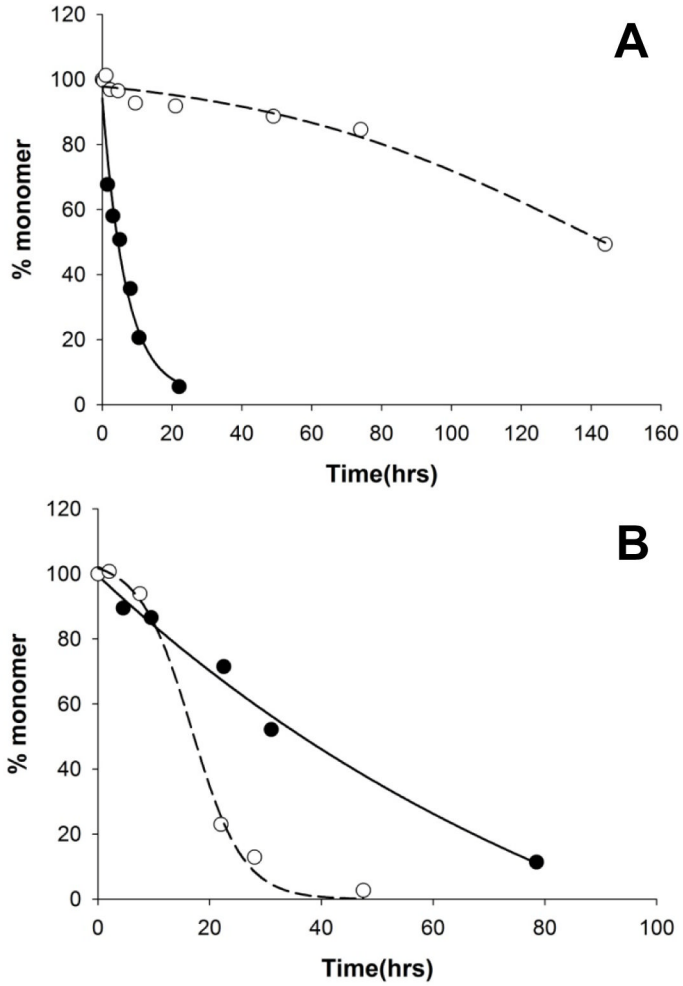

Figure 7.

Kinetics of MF-$Q_{37}P_{10}K_2$ aggregation by the sedimentation assay. (A) Aggregation of 6 μM MF-$Q_{37}P_{10}K_2$ (○) compared to 6 μM $htt^{NT}Q_{37}P_{10}K_2$ (●); (B) aggregation of 31 μM MF-$Q_{37}P_{10}K_2$ (○;) compared to 48 μM $Q_{37}P_{10}K_2$ (●).

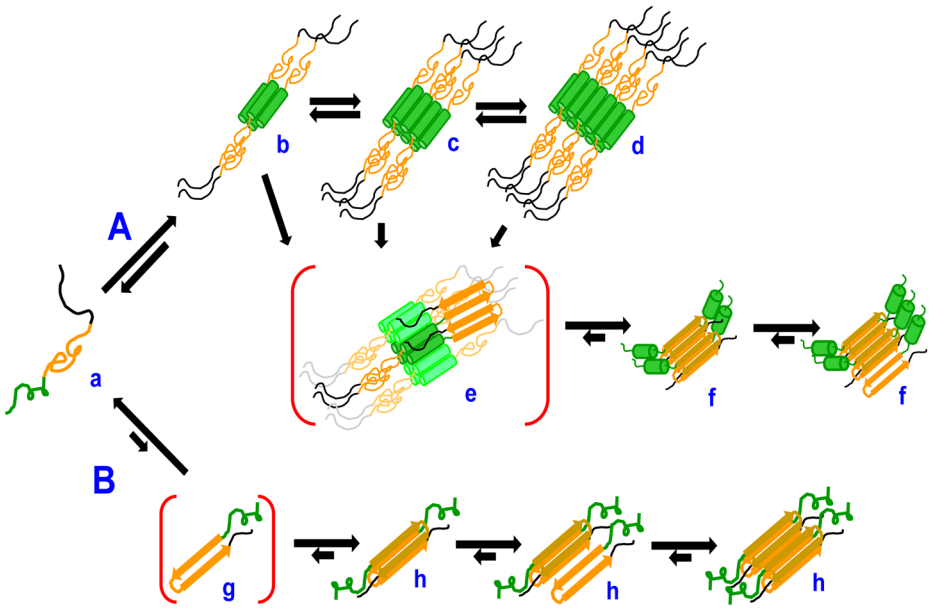

Figure 8.

Kinetically competing pathways for nucleation of amyloid formation in polyQ-containing htt fragments. Monomeric fragment “a” (htt^{NT} = green, polyQ = orange, proline-rich = black) can enter both Pathway A or Pathway B to nucleate amyloid growth, with relative rates depending on structures and conditions. In Pathway A, “a” can reversibly assemble into tetramer “b”, which can further assemble into octomer “c”, dodecamer “d”, and higher order oligomers (not shown). These oligomers are held together primarily via α-helical packing of their htt^{NT} moieties while the polyQ and polyP segments are relatively solvent exposed with no defined structure. Each of “b”, “c” and “d”, as well as higher order oligomers, has a certain propensity to undergo amyloid nucleus (“e”) formation in which some of the attached polyQ sequences assemble into amyloid. Once formed, nucleus “e” can initiate amyloid growth by monomer addition (“f”). In Pathway B, “a” rarely and reversibly undergoes a highly energetically unfavorable folding event to generate a defined conformation or conformations (“g”, the critical nucleus) capable of interacting with the polyQ of another htt fragment to initiate amyloid elongation (“h”). This is a schematic drawing meant to indicate general features of these pathways and structural details, such as the orientation of helices in the tetramer and the packing interfaces in higher oligomers, are yet to be worked out. Likewise, many structural features of the final aggregates of the B pathway and how they relate to the products of the A pathway have not been investigated.